Pergamon

Int. J. Solids Structures Vol. 34, No. 24, pp. 3191–3208, 1997

0020–7683/97 $17.00 + .00

PII: S0020–7683(96)00167–9

HOMOGENIZATION TECHNIQUE AND DAMAGE MODEL FOR OLD MASONRY MATERIAL

RAIMONDO LUCIANO and ELIO SACCO
Department of Industrial Engineering, University of Cassino, Via Zamosch 43-03043 Cassino, Italy

(*Received* 23 *June* 1995; *in revised form* 27 *July* 1996)

Abstract—Masonry is a composite material realized by the inclusion of bricks into the matrix of mortar. In the present paper, a micromechanical approach for defining the properties of a periodic masonry material is proposed. A damage model for old masonries is presented. In fact, it is assumed that the damage is due to the coalescence and growth of the fractures only in the mortar. A repetitive unit cell is chosen and eight possible undamaged and damaged states for the masonry are identified. The homogenization theory for material with periodic microstructure is used to define the overall moduli of the uncracked and cracked masonry. Variational formulations of the periodic problem are given. A numerical procedure for the computation of the elastic properties of the undamaged and damaged masonry material is developed. Then, the damage evolution of the masonry, which accounts for the exact geometry and for the mechanical properties of the constituents of the composite, is obtained. Energy and local strength criteria for the mortar are proposed. The behavior of a typical masonry material is studied and the results are put in comparison with the ones available in the literature. Finally, a simple structural application is developed. © 1997 Elsevier Science Ltd.

1. INTRODUCTION

Many historical buildings and monumental structures are made of masonry material. Hence the analysis of the behavior of masonry structures has always received a great interest from the scientific community.

Two different models, i.e., the continuous model and the discrete block model, have been developed to capture the linear and nonlinear response of the masonry material.

One of the most used continuous model is the so-called no-tension material. According to this model the masonry is indefinitely elastic in compression and cannot support tensile stresses. The no-tension material has been proposed by Heyman (1966), who formulated a theory for the limit analysis of masonry structures. The principal hypothesis is that the tensile strength of the masonry is negligible with respect to the compression strength, and therefore the collapse is generally achieved because of the fractures opening in traction. In the last two decades the no-tension material has been the object of many researches especially in Italy (Como and Grimaldi, 1985; Giaquinta and Giusti, 1985; Romano and Sacco, 1987).

Monumental structures are mostly realized by superimposed blocks. The analysis of these structures is carried out by schematizing the blocks as linear elastic, and the interfaces governed by unilateral with Coulomb friction law. The study of the block structures have been developed by adopting simplified analytical approaches, as for instance in Yim *et al.* (1990), or in conjunction with the finite element method, e.g., Chiostrini and Vignoli (1989), Grimaldi *et al.* (1992) and Lofti and Benson Shing (1994).

A full finite element analysis of a masonry wall which considers the actual microstructure of the material would lead to a very expansive computational problem. In fact, to discretize the mortar joints, a very fine mesh would be considered.

The masonry is a heterogeneous material composed by bricks and mortar disposed in a regular or completely random arrangement. For the most important masonry constructions the adopted material presents a very regular geometry at the microscale level. In fact, the bricks are joined by horizontal and vertical beds of mortar, and generate a periodic microstructure. Hence, the regular masonry material is a periodic composite material. For this reason, some micromechanical methods have been used in order to evaluate the constitutive relationship of the masonry. In particular, in Pande *et al.* (1989) and Kralj *et al.* (1991) the Mori–Tanaka method and the lamination theory have been used in two steps: initially, the Mori–Tanaka method is adopted to define a transition material obtained by neglecting the presence of the horizontal beds of mortar then, the lamination theory is employed for the full homogenization. By following a similar procedure, in Papa (1990) the estimate of the overall moduli of the undamaged masonry has been obtained, and a phenomenological method is employed to model the damage process of the composite material. The two step homogenization procedure (i.e., the Mori–Tanaka method and the lamination theory) have been adopted in Pietruszczak and Niu (1992) and in Gambarotta and Lagomarsino (1994) to study the progressive failure of the structural masonry. Furthermore, the admissible limit surface in the stress space has been carried out in Alpa and Monetto (1994) by schematizing the masonry as blocks in unilateral with friction contact each others, and in De Felice (1994) by taking into account the cohesion between the bricks and the progressive damage of the bricks. The in-plane overall elastic moduli of a masonry have been derived in Anthoine (1995) from the linear elastic constitutive properties of the bricks and the mortar by using the homogenization theory for periodic media in conjunction with the finite element method.

In the present paper, a damage model for ancient masonry material characterized by periodic structures is carried out from a micromechanical analysis. For old masonries the strength of the mortar is lower than the strength of the bricks. Thus, it can be assumed that fractures can develop only in the mortar material (Luciano and Sacco, 1995a). For the periodic unit cell, all the possible states, characterized by different arrangements of cracks in mortar, are identified. Then, for each state of the masonry the corresponding overall moduli are evaluated by imposing periodic boundary conditions on the chosen unit cell. Several variational formulations for media with periodic microstructure are presented. The elastostatic problem, posed in terms of displacements, is approached via finite element method, and new penalty finite elements are proposed in order to enforce on the unit cell periodic boundary conditions. Two strength criteria for the mortar are considered: the first one is based on the energy approach of the elastic fracture mechanics, while the second one corresponds to the local cohesive Coulomb model. Then, the strain limit surfaces for a given masonry material are obtained as function of the specific mechanical characteristics of the mortar. The proposed methodology is implemented in a numerical code. An application for a particular unit cell is developed. The overall elastic moduli for the uncracked and cracked considered material are obtained and compared with results available in literature. The macroscopic limit strain surfaces are presented for both the microscopic strength criteria adopted. Finally, a simple structural example is developed.

2. THE MICROMECHANICAL MODEL OF DAMAGE

Many approaches have been proposed in the literature in order to study the damage process for composites (Talreja, 1987; Laws *et al.* 1983). In particular, the damage available models can be divided in two categories: the phenomenological and the micromechanical models.

In a phenomenological damage scheme the constitutive relationships of the material are deduced only from experimental tests on the composite and, for this reason, many non-physical parameters are necessary to describe the complexity of the phenomenon.

In a micromechanical model the parameters governing the damage process have a physical meaning as, for example, the dimensions, the shapes and the positions of the cracks that characterize the actual damage in the material. Also, in this case, the number of the damage coefficients are very high and for this reason some simplifying hypothesis is often necessary in order to obtain an efficient model. The procedure necessary to define a micromechanical damage model can be summarized in the following steps:

- definition of the geometry of a representative volume element (RVE),
- definition of a damage kinetic law,

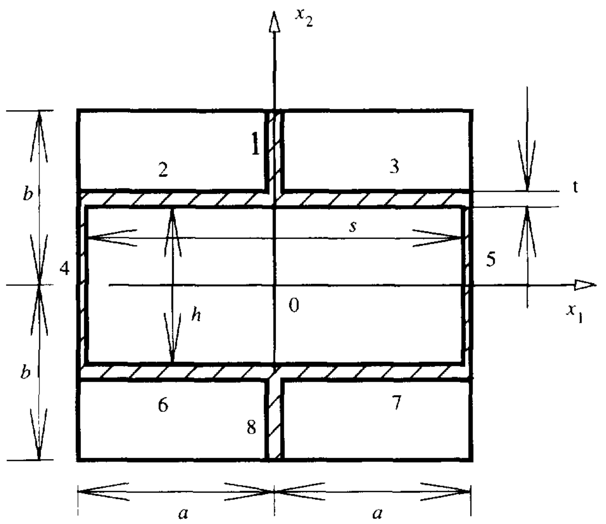

Fig. 1. Repetitive unit cell for the regular masonry material.

- estimate of the global nonlinear behavior of the RVE by using a micromechanical approach of homogenization.

Hence, as first step, the definition of an RVE is required. To this end, it can be noted that the masonry is a composite medium characterized by a regular microstructure: bricks are periodically distributed in the mortar. Consequently, a repetitive cell which encompasses the geometry of the structure and the material properties can be determined. In this way, instead of an RVE, a repetitive cell is employed for the study of the composite material. The chosen unit cell, containing all the geometric and constitutive information on the masonry, is shown in Fig. 1, where each mortar joint is identified by a number. Note that t is the mortar thickness, and s and h the brick sizes. It can be emphasized that the unit cell given in Fig. 1 is not the smallest repetitive cell, but it is suitable for future developments, due to its geometrical simplicity.

Moreover, the damage kinetic law for the material gives the rate of the damage, as function of an evolution parameter (e.g., the time). In the following a damage kinetic law 'discrete' in the time domain is proposed. It is obtained by schematizing the damage process by only a few possible damaged states of the material. In other words, a discrete damage kinetic law is defined by a finite number of fixed damage configurations for the unit cell. Each damaged state or configuration is characterized by a certain distribution of cracks or voids. Furthermore, it is necessary to define the possible paths of damage, i.e., the evolution from a state to another possible one. Obviously, a damage state evolves only to more damaged states, i.e., with a greater number of cracks or voids. Hence, in a discrete damage kinetic law, the constitutive relationship of the material is characterized by a finite number of instantaneous moduli relative to the homogenized response of the unit cell characteristic of all the possible damaged states.

The definition of the discrete damage kinetic law for the masonry arises from the following assumptions:

- the cracks occur only in the mortar material which behaves in a perfect elastic–brittle manner,
- the bricks are indefinitely elastic,
- the mortar thickness is small, so that the cracks can develop only vertically or horizontally,
- when a fracture starts to develop, a full failure of a mortar junction is supposed, i.e. the cracks grow until they reach the blocks.

It can be emphasized, that the proposed damage model captures the behaviour of many masonries. In fact, especially for ancient structures, the tensile strength of the mortar is often much lower than the strength of the bricks, and fractures grow mostly in the mortar.

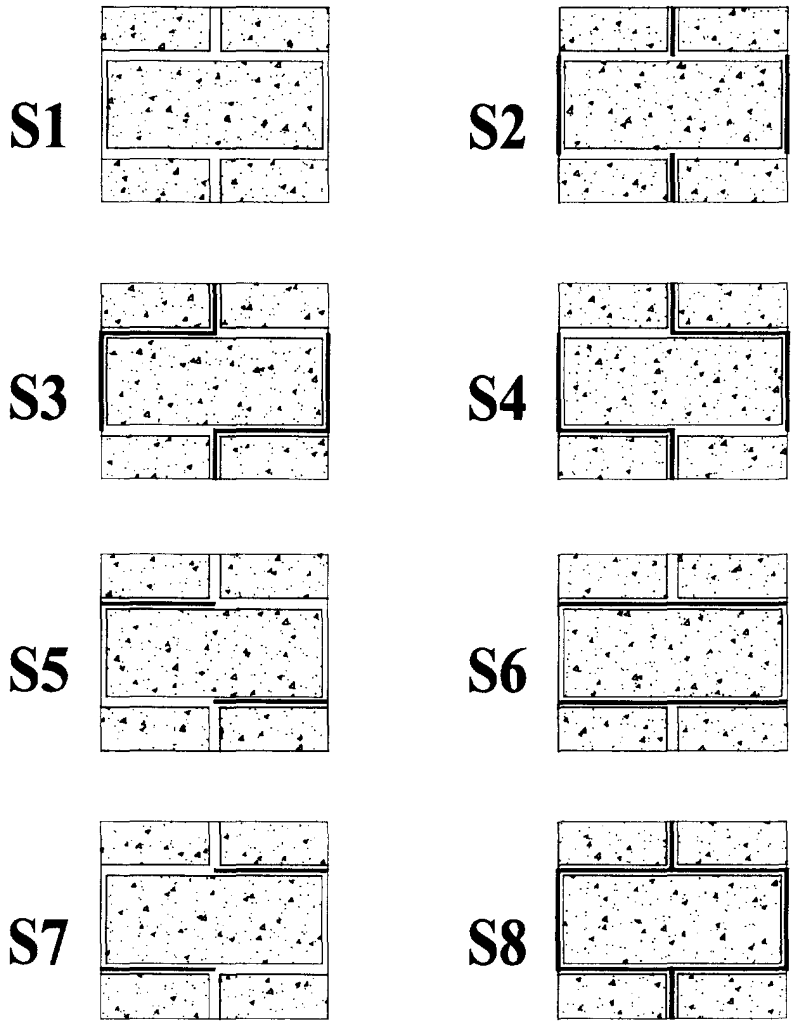

Fig. 2. Possible damaged states of old masonry material.

Table 1. Possible damage paths

Path 1	Path 2	Path 3	Path 4	Path 5	Path 6
S1	S1	S1	S1	S1	S1
S2	S2	S5	S5	S7	S7
S3	S4	S3	S6	S4	S6
S8	S8	S8	S8	S8	S8

During the damage process the fractures should satisfy some simple geometric requirements. In fact, since the unit cell is a repetitive element, then the crack in the joint number 1 is always accompanied by the cracks in the joints numbers 4, 5 and 8. Analogously, cracks in the joint number 2 is always simultaneous to cracks in the joint 7 and crack in the joint 3 occurs with crack in the joint 6. According to these hypotheses, only eight states for the masonry are possible, they are defined by the position of the cracks in the unit cell. In Fig. 2, al the damaged states are schematically represented by indicating the fractures in the mortar by bold lines. In that figure, S1 denotes the undamaged state, and S4 and S5 indicate the mirror states of S3 and S7, respectively. Note that, once the fracture is created, the internal bonds of the mortar material disappear, and cannot be recovered anymore. As a consequence, starting from S1 the damage evolution can follow only six possible paths shown in Table 1. For instance, the unit cell, following the path number 1, evolves from S1 to S2 then to S3 and finally to S8. Moreover, at each damaged state, the fractures can be in open or closed mode. In fact, in compression the fractures are closed and in tension they are open. Consequently, several different situations are possible for each state.

At each damage state of the unit cell it is possible to associate characteristic overall elastic moduli of the masonry material. In fact, the position of the cracks and their state (open or closed) influences the elastic behavior of the unit cell. It is worth noting that the response of the masonry can completely change during the damage process. In fact, the eight states considered are characterized not only by different values of the overall moduli, but also by different material symmetries, as it can be expected for the states S3, S4, S5 and S7.

At this stage, the homogenization theory can be adopted to determine the characteristic overall elastic moduli for each possible state of the masonry in order to define the nonlinear constitutive law of the material.

3. THE HOMOGENIZATION TECHNIQUE

The estimate of the effective elastic moduli of an heterogeneous material can be obtained by using different micromechanical methods (Mura, 1987; Aboudi, 1991). Most of them do not take into account the geometry of the microstructure and the interactions among the blocks are considered approximately. For example, the differential method, the self-consistent or the generalized self-consistent approaches consider the interaction effects by using an iterative numerical procedure; the Mori–Tanaka method adopts the Eshelby solution of an ellipsoidal inclusion in an infinite medium; finally, the dilute scheme does not consider at all the actual microstructure of the heterogeneous material. Further, it has been proposed, by Aboudi, the so-called cell method, which has been extensively discussed and applied to a large number of homogenization problems in the book by Aboudi (1991). This method considers a simplified geometry of the unit cell and, furthermore, assumes a special form for the displacement and stress fields, as emphasized in Teply and Reddy (1991). Many of the micromechanical methods do not allow us to compute the stresses in the composite material. In fact, often they only give the possibility of evaluating the average stress in the matrix and in the inclusions and not the local stresses. Of course, this may represent a limitation in the use of the homogenization techniques, especially when one is interested in the definition of a micromechanical damage model.

Next, a description of the approach to the homogenization technique herein adopted is given. Although some concepts of the proposed homogenization procedure are standard, they are reported in order to make the paper self-consistent. The estimates on the overall in-plane stiffnesses of the masonry are derived from the solution of the inclusion problem characterized by the unit cell V shown in Fig. 1. The problem is treated in the framework of the two-dimensional plain elasticity, and the effects of the transversal stresses ($\sigma_{13}, \sigma_{23}, \sigma_{33}$) in thickness of the masonry wall are not taken into account. On the other hand, the presence of the transversal normal stress σ_{33} in the masonry wall could be responsible for a reduction of its in-plane compressive strength. In fact, as pointed out by Hilsdorf (1969), when the wall is loaded by an in-plane compression, the different deformability of the bricks and the mortar of a masonry wall induces tensile and compressive transversal stresses in the bricks and in the mortar, respectively (Hilsdorf, 1969; Anthoine, 1995). Thus, the traction in the thickness of the bricks could lead to a transversal failure mode of the wall. Since the damage model proposed in the previous section does not consider at all a limited strength in compression, the Hilsdorf effect is not taken into account, and then the two-dimensional approach, although approximate, is consistent with the damage model.

The evaluation of the overall moduli passes throughout the determination of the plain elastic state $\{\mathbf{u}, \varepsilon, \boldsymbol{\sigma}\}$, i.e., the displacement, strain and stress fields solution of the problem governed by the following field equations for heterogeneous media in R^2:

$$
\begin{aligned}
\operatorname{div} \boldsymbol{\sigma}(\mathbf{x}) &= 0 \\
\varepsilon(\mathbf{x}) &= \hat{\nabla} \mathbf{u}(\mathbf{x}) \\
\mathscr{C}(\mathbf{x})\varepsilon(\mathbf{x}) &= \boldsymbol{\sigma}(\mathbf{x})
\end{aligned}
\tag{1}
$$

where $\mathbf{x} = (x_1, x_2)^T$ is the position vector of the typical point of R^2, $\hat{\nabla}$ is the symmetric part of the gradient operator, and $\mathscr{C}(\mathbf{x})$ is the fourth-order constitutive tensor, which is function of the point. Further, the elastic state $\{\mathbf{u}, \boldsymbol{\varepsilon}, \boldsymbol{\sigma}\}$ must satisfy the periodicity and the average condition on the strain. Therefore the displacement field must be represented in the following way (excluding rigid motion) (Suquet, 1982; Anthoine, 1995):

$$\mathbf{u}(\mathbf{x}) = \boldsymbol{\varepsilon}^o \mathbf{x} + \mathbf{u}^p(\mathbf{x}) \tag{2}$$

where $\boldsymbol{\varepsilon}^o$ is the assigned average strain tensor:

$$\boldsymbol{\varepsilon}^o = \langle \boldsymbol{\varepsilon} \rangle = \frac{1}{V} \int_V \boldsymbol{\varepsilon}(\mathbf{x})\, \mathrm{d}x_1\, \mathrm{d}x_2 \tag{3}$$

and $\mathbf{u}^p(\mathbf{x})$ is the part of the displacement vector which is periodic in R^2 with period V and with average on V equal to zero. In Suquet (1982) it has been emphasized that this problem is well posed and admits a unique solution.

The vector $\mathbf{u}^p(\mathbf{x})$ and the tensors $\boldsymbol{\varepsilon}(\mathbf{x})$ and $\boldsymbol{\sigma}(\mathbf{x})$ defining the solution of the problem governed by the eqns (1) and (2), are periodic with period V. As a consequence, they can be regarded as the extension by periodicity in R^2 of the solution of a new problem posed only in V. To formulate the problem only in V, it is necessary to define suitable boundary conditions to impose on ∂V in such a way that the eqns (1) and (2) applied only in V, lead to the restriction in V of the solution of the original elastostatic problem defined in all R^2 (Sanchez-Hubert and Sanchez Palencia, 1992). At this aim, it is important to note that, on ∂V, the solution of the problem posed in R^2 satisfies the following conditions:

$$\begin{aligned} &\text{(a)}\ \boldsymbol{\sigma}(a, x_2)\mathbf{n}(a, x_2) = -\boldsymbol{\sigma}(-a, x_2)\mathbf{n}(-a, x_2) \quad \forall x_2 \in [-b, b] \\ &\text{(b)}\ \boldsymbol{\sigma}(x_1, b)\mathbf{n}(x_1, b) = -\boldsymbol{\sigma}(x_1, -b)\mathbf{n}(x_1, -b) \quad \forall x_1 \in [-a, a] \end{aligned} \tag{4}$$

$$\begin{aligned} &\text{(a)}\ \mathbf{u}^p(a, x_2) = \mathbf{u}^p(-a, x_2) \quad \forall x_2 \in [-b, b] \\ &\text{(b)}\ \mathbf{u}^p(x_1, b) = \mathbf{u}^p(x_1, -b) \quad \forall x_1 \in [-a, a] \end{aligned} \tag{5}$$

which represent the equilibrium and the internal compatibility at the interfaces of adjacent cells, respectively. Hence, the solution of the problem in V must satisfy the eqns (1) and (2) and an opportune combination of the boundary conditions (4) and (5). In particular, it is possible to consider boundary conditions only on the stress (i.e., (4a) and (4b)) or only on the displacement (i.e., (5a) and (5b)), or mixed boundary conditions (i.e., (4a) and (5b) or (4b) and (5a)). Further, in the next section it is proved that when the boundary conditions (5) are used then the (4) are automatically satisfied. In summary, the problem admits a position, traction or mixed boundary conditions. In the following sections only the displacement boundary conditions problem is developed.

Once the periodic elastostatic problem is solved, the components of the effective constitutive tensor $\bar{\mathscr{C}}$ satisfies the classical stress–strain relation for the two-dimensional plane problem at hand, as:

$$\begin{pmatrix} \sigma^o_{11} \\ \sigma^o_{22} \\ \sigma^o_{12} \end{pmatrix} = \begin{pmatrix} \bar{\mathscr{C}}_{1111} & \bar{\mathscr{C}}_{1122} & \bar{\mathscr{C}}_{1112} \\ \bar{\mathscr{C}}_{1122} & \bar{\mathscr{C}}_{2222} & \bar{\mathscr{C}}_{2212} \\ \bar{\mathscr{C}}_{1112} & \bar{\mathscr{C}}_{2212} & \bar{\mathscr{C}}_{1212} \end{pmatrix} \begin{pmatrix} \varepsilon^o_{11} \\ \varepsilon^o_{22} \\ 2\varepsilon^o_{12} \end{pmatrix} \tag{6}$$

where σ^o_{ij} indicates the component of the average on the unit cell of the local stress tensor $\bar{\boldsymbol{\sigma}}$, defined as:

$$\boldsymbol{\sigma}^o = \langle \boldsymbol{\sigma} \rangle = \frac{1}{V}\int_V \boldsymbol{\sigma}\, \mathrm{d}x_1\, \mathrm{d}x_2. \tag{7}$$

The constitutive linear elastic relation (6) is characterized by six constants which can be determined by solving three elastostatic problems. In fact, the typical average strain tensor can be decomposed as reported in the following formula:

$$\varepsilon^o_{ij} = \varepsilon^o_{11}\bar{\varepsilon}^{(1)}_{ij} + \varepsilon^o_{22}\bar{\varepsilon}^{(2)}_{ij} + \varepsilon^o_{12}\bar{\varepsilon}^{(3)}_{ij} \tag{8}$$

where

$$\bar{\boldsymbol{\varepsilon}}^{(1)} = \begin{bmatrix} 1 & 0 \\ 0 & 0 \end{bmatrix} \quad \bar{\boldsymbol{\varepsilon}}^{(2)} = \begin{bmatrix} 0 & 0 \\ 0 & 1 \end{bmatrix} \quad \bar{\boldsymbol{\varepsilon}}^{(3)} = \begin{bmatrix} 0 & 1 \\ 1 & 0 \end{bmatrix}. \tag{9}$$

The overall moduli are then computed as:

$$\begin{aligned} \bar{\mathscr{C}}_{1111} &= \langle \sigma^{(1)}_{11} \rangle \quad \bar{\mathscr{C}}_{1122} = \langle \sigma^{(1)}_{22} \rangle \quad \bar{\mathscr{C}}_{1112} = \langle \sigma^{(1)}_{12} \rangle \\ \bar{\mathscr{C}}_{1122} &= \langle \sigma^{(2)}_{11} \rangle \quad \bar{\mathscr{C}}_{2222} = \langle \sigma^{(2)}_{22} \rangle \quad \bar{\mathscr{C}}_{2212} = \langle \sigma^{(2)}_{12} \rangle \\ \bar{\mathscr{C}}_{1112} &= \langle \sigma^{(3)}_{11} \rangle \quad \bar{\mathscr{C}}_{2212} = \langle \sigma^{(3)}_{22} \rangle \quad \bar{\mathscr{C}}_{1212} = \langle \sigma^{(3)}_{12} \rangle \end{aligned} \tag{10}$$

where $\boldsymbol{\sigma}^{(k)}$ represents the local stress tensor in the unit cell due to the average strain tensor $\bar{\boldsymbol{\varepsilon}}^{(k)}$.

It can be emphasized that the elastostatic problem to solve is not very simple. In fact, difficulties arise in the correct impositions of the conditions (4) and (5), which ensure the periodicity and the continuity of the field variables.

Since the damage evolution of the unit cell is characterized by eight states, it is necessary to derive the corresponding stiffness matrices. At this aim, the previous procedure is applied, and hence, from the solutions of three elastostatic problems for each state, the estimates on the effective elastic moduli of the masonry are derived.

4. BOUNDARY CONDITIONS ON THE DISPLACEMENT FIELD

The aim of this section is the definition of suitable boundary conditions to impose on the displacement variable which condense the eqns (2) and (5). These boundary conditions, associated to the field eqns (1), lead to the solution of the original periodic elastostatic problem.

4.1. *Periodic boundary conditions*

It can be noted that, in order to ensure the continuity of the displacement field between adjacent cells, the conditions (5) are to be satisfied. By taking into account eqn (2), the relations (5) become:

$$\begin{aligned} &\mathbf{u}(a, x_2) - \mathbf{u}(-a, x_2) - \boldsymbol{\varepsilon}^o \begin{Bmatrix} 2a \\ 0 \end{Bmatrix} = 0 \quad \forall x_2 \in [-b, b] \\ &\mathbf{u}(x_1, b) - \mathbf{u}(x_1, -b) - \boldsymbol{\varepsilon}^o \begin{Bmatrix} 0 \\ 2b \end{Bmatrix} = 0 \quad \forall x_1 \in [-a, a]. \end{aligned} \tag{11}$$

The eqns (11) implicitly ensure that the average strain associated to $\mathbf{u}$ is exactly $\boldsymbol{\varepsilon}^o$, as required by the relation (3).

4.2. *Linear boundary conditions*

The displacement condition may be imposed on the boundary ∂V of the unit cell V, according to the formula:

$$\mathbf{u}(\mathbf{x}) = \boldsymbol{\varepsilon}^o \mathbf{x} \quad \text{on}\, \partial V. \tag{12}$$

The boundary condition (12) is stronger than the ones expressed by the eqns (11); in fact, not only does it satisfy the periodicity requirement (2), and hence (5), but it assigns also the value of the displacement along all the boundary.

4.3. *Special cases*

From considerations on the symmetries of both the geometry of the unit cell and the imposed average strain, in some case it is possible to define the boundary conditions ensuring the exact evaluation of some elasticity constant, i.e., satisfying both the conditions (4) and (5). In fact, except for the states S3, S4, S5 and S7, and for the evaluation of the shear modulus for all the possible states, the elasticity components $\bar{\mathscr{C}}_{1111}$ and $\bar{\mathscr{C}}_{1122}$ can be estimated exactly by assuming the following boundary conditions:

$$\begin{array}{lcccc} & x_1 = -a & x_1 = a & x_2 = -b & x_2 = b \\ u_1 = & 0 & 2a & \cdot & \cdot \\ u_2 = & \cdot & \cdot & 0 & 0 \\ \sigma_{12} = & 0 & 0 & 0 & 0 \end{array} \tag{13}$$

while the constants $\bar{\mathscr{C}}_{1122}$ and $\bar{\mathscr{C}}_{2222}$ can be obtained by assuming the following boundary conditions:

$$\begin{array}{lcccc} & x_1 = -a & x_1 = a & x_2 = -b & x_2 = b \\ u_1 = & 0 & 0 & \cdot & \cdot \\ u_2 = & \cdot & \cdot & 0 & 2b \\ \sigma_{12} = & 0 & 0 & 0 & 0 \end{array} \tag{14}$$

where $2a = s+t$ and $b = h+t$.

5. THE NUMERICAL PROCEDURE

As emphasized in Sections 3 and 4, for the evaluation of the overall moduli for all the possible states of the masonry material, several boundary value problems are to be solved. In order to develop numerical procedures for solving the set of elastostatic problems above defined, different variational formulations are presented.

Initially, it is proved that, if the boundary conditions (11) are imposed, the conditions (4) are automatically satisfied, as announced in Section 3. To this end, the Hu–Washizu functional is introduced. For the special problem under consideration with the boundary condition (11) treated as a constraint, the Hu–Washizu functional assumes the form (Washizu, 1976):

$$\Lambda(\mathbf{u},\boldsymbol{\varepsilon},\boldsymbol{\sigma},\boldsymbol{\lambda}^{(a)},\boldsymbol{\lambda}^{(b)}) = \frac{1}{2}\int_V \mathscr{C}\boldsymbol{\varepsilon}\cdot\boldsymbol{\varepsilon}\,\mathrm{d}x_1\,\mathrm{d}x_2 - \int_V \boldsymbol{\sigma}\cdot\boldsymbol{\varepsilon}\,\mathrm{d}x_1\,\mathrm{d}x_2 + \int_V \hat{\nabla}\mathbf{u}\cdot\boldsymbol{\sigma}\,\mathrm{d}x_1\,\mathrm{d}x_2$$
$$- \int_{-b}^{b}\left[\boldsymbol{\lambda}^{(a)}\cdot\left(\mathbf{u}(a,x_2) - \mathbf{u}(-a,x_2) - \boldsymbol{\varepsilon}^0\begin{Bmatrix}2a\\0\end{Bmatrix}\right)\right]\mathrm{d}x_2$$

$$-\int_{-a}^{a}\left[\boldsymbol{\lambda}^{(b)}\cdot\left(\mathbf{u}(x_1,b)-\mathbf{u}(x_1,-b)-\boldsymbol{\varepsilon}^0\begin{Bmatrix}0\\2b\end{Bmatrix}\right)\right]\mathrm{d}x_1 \qquad (15)$$

where $\boldsymbol{\lambda}^{(a)}$ and $\boldsymbol{\lambda}^{(b)}$ are the Lagrange multipliers associated to the constraints (11). The stationary conditions for Λ with respect to $\boldsymbol{\sigma}$ and $\boldsymbol{\varepsilon}$ lead to the compatibility and the constitutive eqns $(1)_2$ and $(1)_3$, respectively. The stationary conditions for Λ with respect to $\boldsymbol{\lambda}^{(a)}$ and $\boldsymbol{\lambda}^{(b)}$ lead to the constraint eqns (11). The stationary condition with respect to $\mathbf{u}$ leads to:

$$-\int_V \delta\mathbf{u}\cdot\operatorname{div}\boldsymbol{\sigma}\,\mathrm{d}x_1\,\mathrm{d}x_2+\int_{-b}^{b}[\delta\mathbf{u}\cdot(\boldsymbol{\sigma}\mathbf{n}-\boldsymbol{\lambda}^{(a)})]_{x_1=a}\,\mathrm{d}x_2-\int_{-b}^{b}[\delta\mathbf{u}\cdot(\boldsymbol{\sigma}\mathbf{n}+\boldsymbol{\lambda}^{(a)})]_{x_1=-a}\,\mathrm{d}x_2$$
$$-\int_{-a}^{a}[\delta\mathbf{u}\cdot(\boldsymbol{\sigma}\mathbf{n}-\boldsymbol{\lambda}^{(b)})]_{x_2=b}\,\mathrm{d}x_1-\int_{-a}^{a}[\delta\mathbf{u}\cdot(\boldsymbol{\sigma}\mathbf{n}+\boldsymbol{\lambda}^{(b)})]_{x_2=-b}\,\mathrm{d}x_1=0. \qquad (16)$$

Note that this equation carries the equilibrium field eqn $(1)_1$, and further it allows to determine the values of the Lagrange multipliers as:

$$\begin{aligned}[\boldsymbol{\sigma}\mathbf{n}]_{x_1=a}-\boldsymbol{\lambda}^{(a)}&=0\\ [\boldsymbol{\sigma}\mathbf{n}]_{x_1=-a}+\boldsymbol{\lambda}^{(a)}&=0\\ [\boldsymbol{\sigma}\mathbf{n}]_{x_2=b}-\boldsymbol{\lambda}^{(b)}&=0\\ [\boldsymbol{\sigma}\mathbf{n}]_{x_2=-b}+\boldsymbol{\lambda}^{(b)}&=0.\end{aligned} \qquad (17)$$

The mechanical meaning of the $\boldsymbol{\lambda}$'s clearly appears. They represent the stress at interface between two adjacent cells. Thus, because of the relations (17), it is proved that when the constraint (11) is imposed in the variational formulation, the equations (4) are automatically satisfied. Finally, it can be concluded that the stationary conditions for the functional (15) are equivalent to all the equations governing the original elastostatic problem posed in V.

Now, let the boundary condition (12) be considered. In this case, the constrained Hu–Washizu functional turns out to be:

$$\tilde{\Lambda}(\mathbf{u},\boldsymbol{\varepsilon},\boldsymbol{\sigma},\boldsymbol{\eta})=\frac{1}{2}\int_V \mathscr{C}\boldsymbol{\varepsilon}\cdot\boldsymbol{\varepsilon}\,\mathrm{d}x_1\,\mathrm{d}x_2-\int_V \boldsymbol{\sigma}\cdot\boldsymbol{\varepsilon}\,\mathrm{d}x_1\,\mathrm{d}x_2$$
$$+\int_V \hat{\nabla}\mathbf{u}\cdot\boldsymbol{\sigma}\,\mathrm{d}x_1\,\mathrm{d}x_2-\int_{-b}^{b}\int_{\partial V}[\boldsymbol{\eta}\cdot(\mathbf{u}-\boldsymbol{\varepsilon}^o\mathbf{x})]\,\mathrm{d}x_2 \qquad (18)$$

where $\boldsymbol{\eta}$ is the Lagrange multiplier of the constraint (12). The stationary conditions for $\tilde{\Lambda}$ with respect to $\boldsymbol{\sigma}$ and $\boldsymbol{\varepsilon}$ yield the eqns $(1)_2$ and $(1)_3$, respectively. The stationary condition for $\tilde{\Lambda}$ with respect to $\boldsymbol{\eta}$ yields the constraints equation (12). Finally, the stationary condition for $\tilde{\Lambda}$ with respect to $\mathbf{u}$ leads to:

$$-\int_V \delta\mathbf{u}\cdot\operatorname{div}\boldsymbol{\sigma}\,\mathrm{d}x_1\,\mathrm{d}x_2+\int_{\partial V}[\delta\mathbf{u}\cdot(\boldsymbol{\sigma}\mathbf{n}-\boldsymbol{\eta})]\,\mathrm{d}s=0. \qquad (19)$$

It gives the equilibrium eqn $(1)_1$, and allows to determine the values of the Lagrange multipliers as the stress on the boundary of the cell. Contrarily to the previous case, when the constraint (11) is enforced, by employing the functional (18), the eqns (4) could not be satisfied.

From a computational point of view the approach via the Lagrangian mixed functional is not very effective, because of the high number of unknown functions involved. Hence, a full displacement formulation appears suitable. By satisfying the eqns $(1)_2$ and $(1)_3$ and by enforcing the constraint (11) via penalty method, the functional (15) gives the penalized potential energy:

$$\pi(\mathbf{u}) = \frac{1}{2}\int_{\Omega} \mathscr{C}(\mathbf{x})\hat{\nabla}\mathbf{u}(\mathbf{x})\cdot\hat{\nabla}\mathbf{u}(\mathbf{x})\,\mathrm{d}x_1\,\mathrm{d}x_2 + \frac{\kappa}{2}\int_{-b}^{b}\left\| \mathbf{u}(a,x_2)-\mathbf{u}(-a,x_2)-\boldsymbol{\varepsilon}^o\begin{Bmatrix}2a\\0\end{Bmatrix}\right\|^2 \mathrm{d}x_2$$
$$+\frac{\kappa}{2}\int_{-a}^{a}\left\|\mathbf{u}(x_1,b)-\mathbf{u}(x_1,-b)-\boldsymbol{\varepsilon}^o\begin{Bmatrix}0\\2b\end{Bmatrix}\right\|^2 \mathrm{d}x_1 \quad (20)$$

which is the potential energy augmented by two penalty terms corresponding to the boundary conditions (11). The quantity κ in formula (20) is the penalty parameter, which should assume a very high value to well enforce the desired boundary conditions. Because of eqn (2), the penalized potential energy (20) can be rewritten as function of only the periodic part of the displacement field $\mathbf{u}^p(\mathbf{x})$. In this case, the functional π^p is determined as:

$$\pi^p(\mathbf{u}^p) = \frac{1}{2}\int_{\Omega} \mathscr{C}(\mathbf{x})\hat{\nabla}\mathbf{u}^p(\mathbf{x})\cdot\hat{\nabla}\mathbf{u}^p(\mathbf{x})\,\mathrm{d}x_1\,\mathrm{d}x_2 + \frac{\kappa}{2}\int_{-b}^{b}\|\mathbf{u}^p(a,x_2)-\mathbf{u}^p(-a,x_2)\|^2\,\mathrm{d}x_2$$
$$+\frac{\kappa}{2}\int_{-a}^{a}\|\mathbf{u}^p(x_1,-b)-\mathbf{u}^p(x_1,-b)\|^2\,\mathrm{d}x_1. \quad (21)$$

The stationary condition for the functionals (20) and (21) gives the total displacement $\mathbf{u}$ or the periodic displacement $\mathbf{u}^p$, approximate solutions of the periodic elastostatic problem.

The discretization of the penalized potential energies (20) and (21) involves the definition of new penalty elements, which are very important because they contain the boundary information. Note that the average strain condition is contained in the penalty terms for the functional (20) and, as emphasized above, in the strain energy term for the functional (21). In the first case, the imposed strain average is regarded as contact distributed forces on the boundary of the unit cell, in the latter case the effect of $\boldsymbol{\varepsilon}^o$ corresponds to assigned body forces.

6. THE STRENGTH OF THE MASONRY

In this section, two macroscopic damage laws for the homogenized material are deduced from the micromechanical approach. They are based on the strength of the mortar material. In fact, as specified in Section 2, the only constituent of the composite which is responsible for the damage is the mortar.

During the application of the external loading on the masonry structure, the typical point is subjected to a stress and strain evolution. As a consequence, the unit cell, which represents in the microscale the point of the macroscale, also undergoes to a deformation process, which can induce the coalescence and the growth of fractures. Further, note that the mean strain $\boldsymbol{\varepsilon}^o$ and the mean stress $\boldsymbol{\sigma}^o$ in the unit cell, are the actual strain and stress in the point of the macroscale.

6.1. *The energy criterion*

By applying the concepts of the elastic fracture mechanics, a crack in the unit cell grows if its strain energy release rate per unit of area is equal to greater than the limit Griffith G energy per unit of area, in other words:

Table 2. Crack sizes l for the possible damage paths

Path 1 & 2	Path 3 & 5	Path 4 & 6
$3h+6t$	$s+t$	$s+t$
$s+t$	$3h+6t$	$s+t$
$s+t$	$s+t$	$3h+6t$

$$\Gamma = -\frac{d}{dl}\mathscr{U}(l) < G \quad \text{there is not crack growth}$$

$$\Gamma = -\frac{d}{dl}\mathscr{U}(l) \geqslant G \quad \text{there is crack growth} \tag{22}$$

where l measures the total length of the fractures in the actual state and $\mathscr{U}(l)$ is the density (fracture) strain energy of the unit cell. On the base of the possible cracked states presented in Section 2, a simplified approach based on the fracture mechanics is developed. In practice, the energy release rate is computed by substituting to the derivative of the strain energy, the incremental ratio of the strain energy. Hence the crack growth criterion becomes:

$$\Gamma = -\frac{\mathscr{U}(l+\Delta l)-\mathscr{U}(l)}{\Delta l} < G \quad \text{there is not crack growth}$$

$$\Gamma = -\frac{\mathscr{U}(l+\Delta l)-\mathscr{U}(l)}{\Delta l} \geqslant G \quad \text{there is crack growth} \tag{23}$$

where the increment of the crack propagation Δl can be determined from the difference between the length l of the fracture in the actual state and the one in the next possible state. Hence, in Table 2 the values of the size of the crack growth are given for the six possible paths of damage proposed in Section 2.

The fracture strain energy of the unit cell per unit of area is assumed as the elastic energy associated to the part of the strain responsible for the crack growth (Luciano and Sacco, 1995a). As a matter of fact, if the unit cell is subjected to a biaxial average compressive strain state, then the fracture does not occur. On the contrary, for an elongation in the x_1-direction, the cell could pass from the initial state S1 to S2. From a mechanical point of view, it can be assumed that the positive normal strains ε^o_{11} and ε^o_{22} acting along the x_1- and x_2-directions, respectively, could induce fracture growth. Further, it can be supposed that also the shear strain ε^o_{12} could be responsible for fracture openings. In those hypotheses, the choice for the fracture strain energy, associated to a dimension l of the crack state, is the following:

$$\mathscr{U}(l;\boldsymbol{\varepsilon}^o) = \tfrac{1}{2}(\mathscr{C}(l)\boldsymbol{\varepsilon}^{0-}\cdot\boldsymbol{\varepsilon}^{0+}) \tag{24}$$

where $\boldsymbol{\varepsilon}^{0+}$ is obtained from the strain tensor $\boldsymbol{\varepsilon}^o$ by neglecting the negative part of the components ε^o_{11} and ε^o_{22}. Explicitly, it is:

$$\text{if}\,\varepsilon^o_{11} > 0 \quad \text{and} \quad \varepsilon^o_{22} > 0 \quad \boldsymbol{\varepsilon}^{0+} = \begin{bmatrix} \varepsilon^o_{11} & \varepsilon^o_{12} \\ \varepsilon^o_{12} & \varepsilon^o_{22} \end{bmatrix}$$

$$\textit{if}\,\varepsilon^o_{11} > 0 \quad \text{and} \quad \varepsilon^o_{22} \leqslant 0 \quad \boldsymbol{\varepsilon}^{0+} = \begin{bmatrix} \varepsilon^o_{11} & \varepsilon^o_{12} \\ \varepsilon^o_{12} & 0 \end{bmatrix}$$

$$\textit{if}\,\varepsilon^o_{11} \leqslant 0 \quad \text{and} \quad \varepsilon^o_{22} \leqslant 0 \quad \boldsymbol{\varepsilon}^{0+} = \begin{bmatrix} 0 & \varepsilon^o_{12} \\ \varepsilon^o_{12} & 0 \end{bmatrix}. \tag{25}$$

Note that the constitutive stiffness matrix $\bar{\mathscr{C}}(l)$ contained the overall moduli of the actual damage state carried out by following the procedure developed in Section 5.

6.2. *The cohesive Coulomb criterion*

According to formula (8), the local stress tensor in a typical point of the cell is given by:

$$\sigma_{ij} = \varepsilon^o_{11}\sigma^{(1)}_{ij} + \varepsilon^o_{22}\sigma^{(2)}_{ij} + \varepsilon^o_{12}\sigma^{(3)}_{ij}. \tag{26}$$

In particular, by using eqn (26), it is possible to compute the stress state at the middle point of each mortar layer, previously singled out by the numbers from 1 to 8, as shown in Fig. 1. At each mortar joint the crack opening depends on the values of the normal σ_n and tangential τ stresses. The normal stress is $\sigma_n = \sigma_{22}$ for horizontal mortar joints and $\sigma_n = \sigma_{11}$ for vertical mortar joints, while the tangential stress is always given by $\tau = \sigma_{12}$. Of course, the normal and the tangential stresses are computed in the middle point of the joints where there is not yet crack. Furthermore, as pointed out in Section 2, symmetry considerations allow to say:

$$\begin{aligned} \sigma_{ij}(P_1) = \sigma_{ij}(P_4) = \sigma_{ij}(P_5) &= \sigma_{ij}(P_8) \\ \sigma_{ij}(P_2) &= \sigma_{ij}(P_7) \\ \sigma_{ij}(P_3) &= \sigma_{ij}(P_6) \end{aligned} \tag{27}$$

where P_i indicates the middle point of the ith mortar layer. It can be emphasized that P_1 has coordinates: $x_1 = 0$, $x_2 = a$. As consequence of the identities (27), it is sufficient to compute the tangential and normal stresses at only three points in the cell, say at P_1, P_2 and P_3.

From the value of the stresses (σ_n, τ), it is possible to determine, by means of a local limit strength criterion, which one of the mortar layer reaches the limit state, and hence where the new crack opening is localized. Of course, it is fundamental the choice of a local limit strength criterion. The very simple cohesive Coulomb criterion is considered herein, which states that a couple (σ_n, τ) is strictly admissible if it satisfies the relationships:

$$\begin{cases} c - \sigma_n > 0 \\ |\tau| < \mu(c - \sigma_n) \end{cases} \tag{28}$$

where μ is the friction coefficient and c is the cohesive stress of the mortar. Because of the relation (26), the limit surface, i.e., the set of couples (σ_n, τ) satisfying eqns (28) in the limit sense, is obtained as the internal envelope of the following equations:

$$\begin{cases} \varepsilon^o_{11}\sigma^{(1)}_n(P_i) + \varepsilon^o_{22}\sigma^{(2)}_n(P_i) + \varepsilon^o_{12}\sigma^{(3)}_n(P_i) \leqslant c \\ \quad \mu c = \varepsilon^o_{11}(\pm\tau^{(1)}(P_i) + \mu\sigma^{(1)}_n(P_i)) \\ \quad\quad + \varepsilon^o_{22}(\pm\tau^{(2)}(P_i) + \mu\sigma^{(2)}_n(P_i)) \\ \quad\quad + \varepsilon^o_{12}(\pm\tau^{(3)}(P_i) + \mu\sigma^{(3)}_n(P_i)) \end{cases} . \tag{29}$$

Finally, the eqns (29) in the strain space spanned by $(\varepsilon^o_{11}, \varepsilon^o_{22}, \varepsilon^o_{12})$ furnish the macroscopic limit deformation surface.

7. MATERIAL AND STRUCTURAL APPLICATIONS

Next, the proposed procedure is applied by using the finite element method in order to determine the material behavior and to develop a simple structural application. The unit cell considered is characterized by the following dimensions: $h = 75$ mm, $s = 225$ mm and

Table 3. Elastic moduli for the undamaged masonry

Moduli (MPa)	C_{1111}	C_{2222}	C_{1122}	C_{1212}
Boundary conditions (11)	8942	5595	1578	1562
Boundary conditions (12)	10,029	5944	1743	2061
Boundary conditions (13)–(14)	8942	5600	1580	—
Solution in Kralj *et al.* (1991)	8242	5593	1504	1521
Lower bound in Luciano (1995)	8665	5643	1600	1521
Upper bound in Luciano (1995)	10,165	6655	3081	1952

Table 4. Overall elastic moduli for undamaged and damaged states

Moduli (MPa)	S1	S2	S3	S4	S5	S6	S7	S8
C_{1111}	8942	2761	1203	1203	8398	7967	8398	0
C_{2222}	5595	5329	381	381	1343	0	1343	0
C_{1212}	1562	1326	654	654	838	0	838	0
C_{1122}	1578	630	677	677	530	0	530	0
C_{1112}	0	0	887	−887	−386	0	386	0
C_{2212}	0	0	499	−499	−202	0	202	0

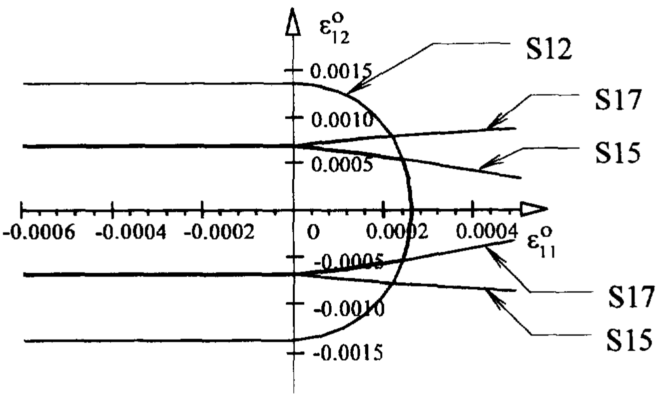

Fig. 3. Limit surface for the state S1, when $\varepsilon_{22}^{o} = 0$, obtained by using the energy criterion.

$t = 15$ mm (see Fig. 1). The matrix (m) and the blocks (b) are isotropic with elastic moduli: $E_b = 15{,}000$ MPa, $\nu_b = 0.25$, $E_m = 1000$ MPa, and $\nu_m = 0.3$. These values are equal to the ones adopted in Kralj *et al.* (1991). The plain strain elastostatic analysis of the unit cell is carried out by using a finite element program and a mesh with 6932 isoparametric four node elements. Further, the boundary conditions on the displacement defined in Section 4, are adopted.

First, the state S1 is analyzed and the corresponding elastic moduli are estimated by adopting the boundary conditions defined by eqns (11) or the ones given in (12), (13) and (14). In Table 3, they are put in comparison with the results obtained in Kralj *et al.* (1991) and with the bounds proposed by Luciano (1995). It can be emphasized the good agreement of the numerical results obtained.

Successively, all the possible states are studied by solving the problem of the stationary for the functional (20), which accounts for the boundary conditions (11) via penalization. The results obtained are given in Table 4.

Once the elastic moduli for each state are known, the proposed energy criterion is applied to the case under consideration. In the following, the limit energy $G = 0.007$ MPa is taken. The limit surfaces relative to the damage evolution from the state S1 to the states S2, S5 and S7 are represented for the case $\varepsilon_{22}^{o} = 0$ in Fig. 3 and for the case $\varepsilon_{11}^{o} = 0$ in Fig. 4. Then, the limit surfaces relative to the damage evolution of the state S2 to the states S3 and S4 are reported for $\varepsilon_{22}^{o} = 0$ in Fig. 5 and for $\varepsilon_{22}^{o} = 0.0002$ in Fig. 6. From the analysis of Figs 3–6, the effective limit surface for the possible damage evolution from state S1 or

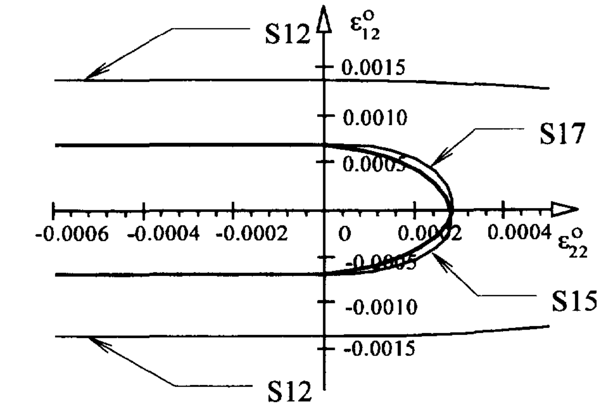

Fig. 4. Limit surface for the state S1, when $\varepsilon^o_{11} = 0$, obtained by using the energy criterion.

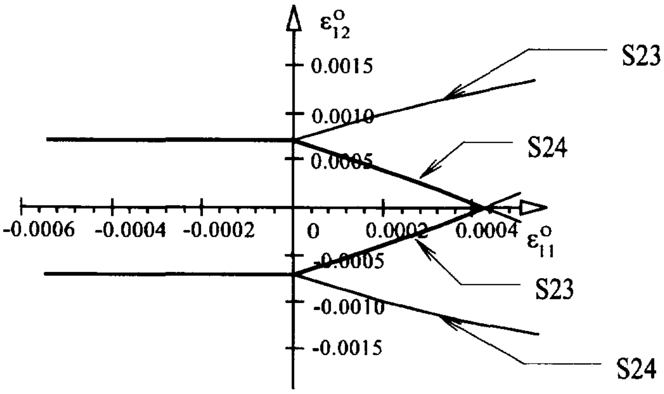

Fig. 5. Limit surface for the state S2, when $\varepsilon^o_{22} = 0$, obtained by using the energy criterion.

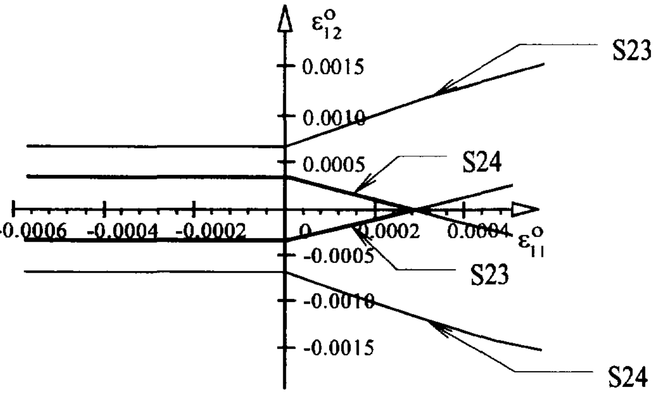

Fig. 6. Limit surface for the state S2, when $\varepsilon^o_{22} = 0.0002$, obtained by using the energy criterion.

S2 clearly appears as the internal envelope of the curves S12, S15 and S17 or the internal envelope of the curves S23 and S24. Note that with *Sij* it is denoted the limit surface from the state *Si* to the state *Sj*.

Then, the local cohesive Coulomb criterion is employed. The friction coefficient and the cohesion strength of the mortar are assumed, $\mu = 2$ and $c = 225$ MPa, respectively. For the considered problem, the values of the stresses for all the possible state of the masonry are given in Tables 5, 6 and 7 at the points P_1, P_2 and P_3. Analogously to the results presented when the damage energy criterion is adopted, also for the cohesive local criterion the limit surfaces relative to the damage evolution from the state S1 to the states S2, S5 and S7 are plotted for the case $\varepsilon^o_{22} = 0$ in Fig. 7 and for the case $\varepsilon^o_{11} = 0$ in Fig. 8. Then, the limit surfaces relative to the damage evolution of the state S2 to the states S3 and S4 are reported for $\varepsilon^o_{22} = 0$ in Fig. 9 and for $\varepsilon^o_{22} = 0.0002$ in Fig. 10. The effective limit surface

Table 5. Stresses in the points P_1, P_2 and P_3 due to the average strain tensor $\bar{\varepsilon}^{(1)}$

Stresses (MPa)	S1	S2	S3	S4	S5	S6	S7	S8
$\sigma_n(P_1)$	9113	0	0	0	9260	9520	9260	0
$\tau(P_1)$	0	0	0	0	163	0	−163	0
$\sigma_n(P_2)$	1248	340	0	880	452	0	0	0
$\tau(P_2)$	−960	−2050	0	−1830	−995	0	0	0
$\sigma_n(P_3)$	1248	340	880	0	0	0	452	0
$\tau(P_3)$	960	2050	1830	0	0	0	995	0

Table 6. Stresses in the points P_1, P_2 and P_3 due to the average strain tensor $\bar{\varepsilon}^{(2)}$

Stresses (MPa)	S1	S2	S3	S4	S5	S6	S7	S8
$\sigma_n(P_1)$	927	0	0	0	4	0	4	0
$\tau(P_1)$	0	0	0	0	1690	0	−1690	0
$\sigma_n(P_2)$	5818	5670	0	495	1854	0	0	0
$\tau(P_2)$	−77	−231	0	−1034	−446	0	0	0
$\sigma_n(P_3)$	5818	5670	495	0	0	0	1854	0
$\tau(P_3)$	77	231	1034	0	0	0	446	0

Table 7. Stresses in the points P_1, P_2 and P_3 due to the average strain tensor $\bar{\varepsilon}^{(3)}$

Stresses (MPa)	S1	S2	S3	S4	S5	S6	S7	S8
$\sigma_n(P_1)$	0	0	0	0	885	0	−885	0
$\tau(P_1)$	1580	0	0	0	1020	0	1020	0
$\sigma_n(P_2)$	−483	−874	0	−1320	−583	0	0	0
$\tau(P_2)$	3070	2696	0	2750	3240	0	0	0
$\sigma_n(P_3)$	483	874	1320	0	0	0	583	0
$\tau(P_3)$	3070	2696	2750	0	0	0	3240	0

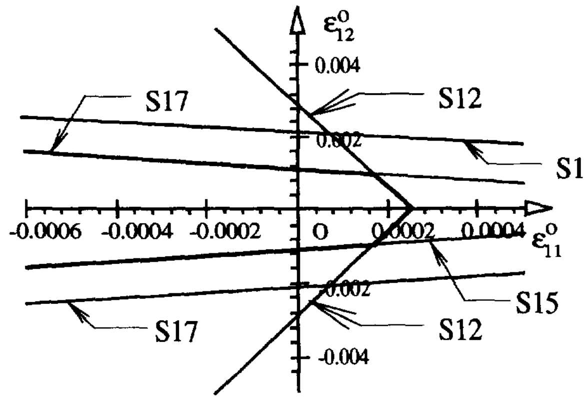

Fig. 7. Limit surface for the state S1, when $\varepsilon_{22}^{o} = 0$, obtained by using the cohesive local criterion.

for the possible damage evolution from state S1 or from the state S2 clearly appears as the internal envelope of the presented curves.

Finally, a structural application is developed. It consists in the masonry wall represented in Fig. 11, subjected to a uniformly distributed vertical load $q = 220$ kN/m and to an increasing horizontal displacement u at each point of the top. The dimensions of the wall are: $L = 5$ m and $H = 6$ m. The material properties corresponding to the cohesive Coulomb criterion previously carried out, are adopted. The numerical procedure developed for solving the nonlinear problem governed by the described discrete damage evolution law is presented in Luciano and Sacco (1995b). In Fig. 12 the plot of the values of the total horizontal force F acting on the top of the wall vs u, is given. The brittle behavior of the structure can be noted. Furthermore, in Fig. 11 the distribution of the masonry states is

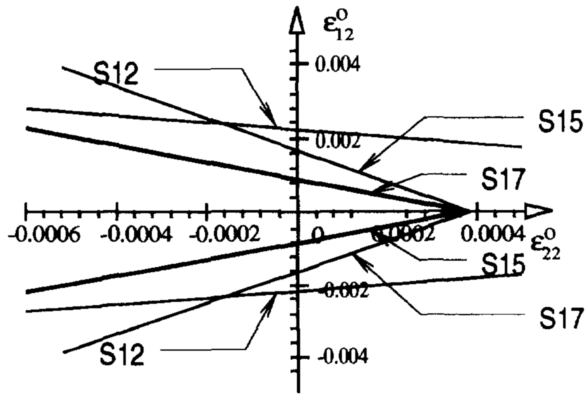

Fig. 8. Limit surface for the state S1, when $\varepsilon^o_{11} = 0$, obtained by using the cohesive local criterion.

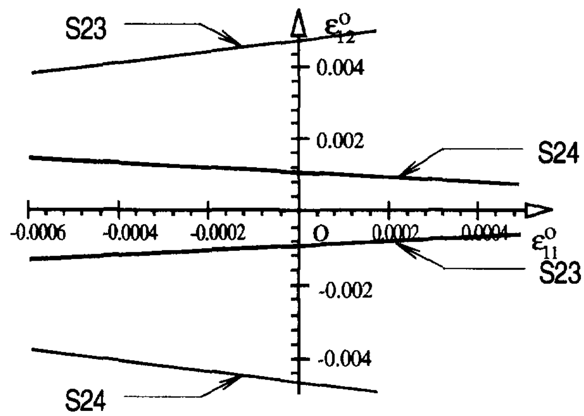

Fig. 9. Limit surface for the state S2, when $\varepsilon^o_{22} = 0$, obtained by using the cohesive local criterion.

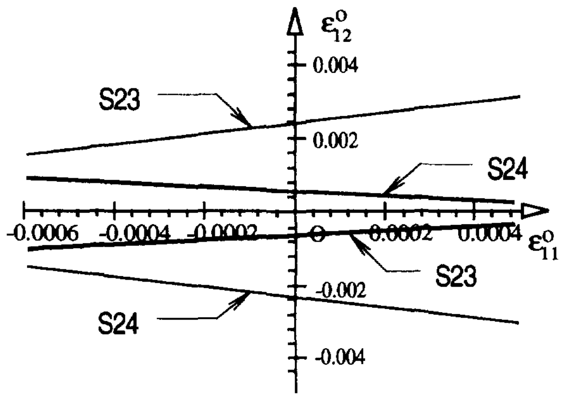

Fig. 10. Limit surface for the state S2, when $\varepsilon^o_{22} = 0.0002$, obtained by using the cohesive local criterion.

reported when the applied displacement is u_A (see Fig. 12). The opening of horizontal fractures is due to the bending of the wall.

8. CONCLUSIONS

A discretized damage model for the masonry material has been obtained by solving the micro-macro problem, i.e., the macromechanical damage model has been determined by using the micromechanics and the homogenization theory. The damage model obtained appears simple and able to capture the behavior of many regular masonry materials.

Variational formulations have been presented. In particular, the Hu–Washizu functionals for the two possible boundary conditions on the unit cell have been reported. By

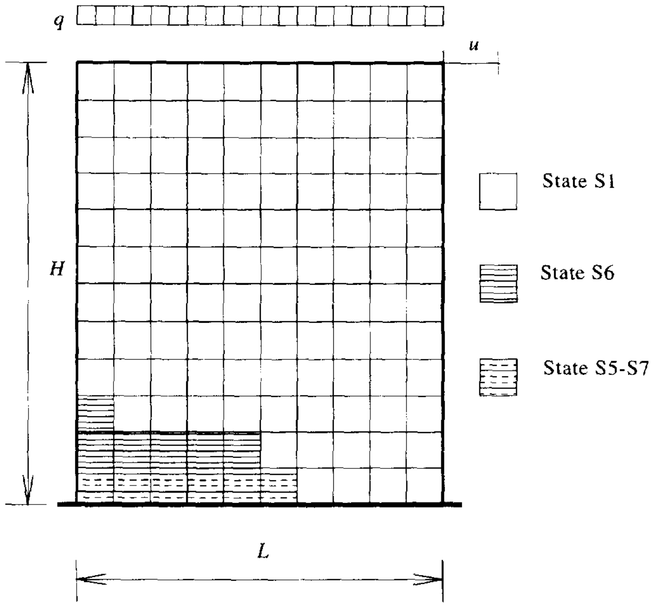

Fig. 11. Masonry wall subjected to a vertical distributed load q and to a horizontal displacement u on the top.

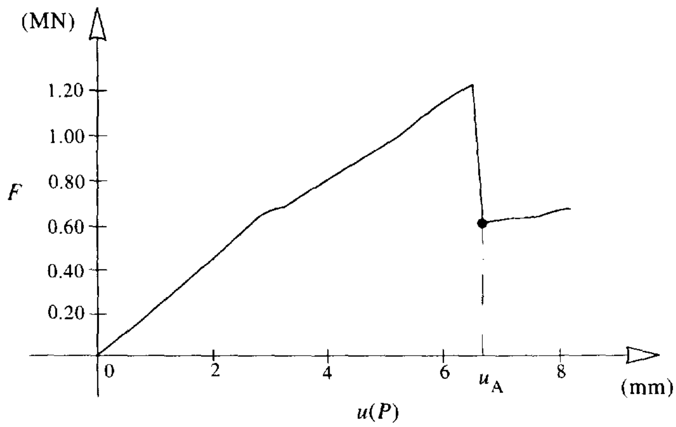

Fig. 12. Total horizontal force F acting on the top of the wall vs the applied displacement u.

means of the Hu–Washizu formulation, it has been proved that, by imposing the continuity of the periodic part of the displacement, the continuity of the stress is automatically satisfied. Then, a handy penalty displacement formulation has been presented, and its finite element implementation has been developed.

Two strength criteria for the mortar have been adopted. Since the procedure proposed allows to determine the whole elastic state in the unit cell, it can be emphasized that any other type of local strength criterion can be adopted in the model. The effectiveness of the proposed damage model has been tested by developing a simple structural application.

Acknowledgements—The financial supports of the Italian National Research Council (CNR) and Ministry of University and Research (MURST) are gratefully acknowledged.

REFERENCES

Aboudi, J. (1991). *Mechanics of Composite Materials*, Elsevier, Oxford.

Alpa, G. and Monetto, I. (1994). Microstructural model for dry block masonry walls with in-plane loading. *Journal of the Mechanics and Physics of Solids* **42**, 1159–1175.

Anthoine, A. (1995). Derivation of the in-plane elastic characteristics of masonry through homogenization theory. *International Journal of Solids and Structures* **32**, 137–163.

Chiostrini, S. and Vignoli, A. (1989). Application of a numerical method to the study of masonry panels with various geometry under seismic loads. In *Structural Repair and Maintenance of Historical Buildings* (ed. C. A. Brebbia), Computational Mechanics Publications.

Como, M. and Grimaldi, A. (1985). A unilateral model for the limit analysis of masonry walls. In *Unilateral Problems in Structural Analysis* (eds G. Del Piero and F. Maceri), CISM Courses and Lectures, Vol. 288, pp. 25–45. Springer-Verlag, Berlin.

De Felice, G. (1994). Failure criterion for brick masonry under in plane load: a micromechanical approach. In *U.S.–Italian Workshop on Guidelines for Seismic Evaluation and Rehabilitation of Unreinforced Masonry Buildings* (eds D. P. Abrams and G. M. Calvi), Report NCEER-94-0021, State University of New York at Buffalo.

Gambarotta, L. and Lagomarsino, S. (1994). Damage in brick masonry shear walls. In *Fracture and Damage in Quasibrittle Structures: Experiments, Modelling and Computer Analysis* (eds Z. P. Bazant, Z. Bittnar, M. Jirasek and J. Mazars), pp. 463–472, E & FN Spon.

Giaquinta, M. and Giusti, E. (1985). Researches on the equilibrium of masonry structures. *Archives of Rational Mechanics Analysis* **88,** 359–392.

Grimaldi, A., Luciano, R. and Sacco, E. (1992). Nonlinear dynamic analysis of masonry structures via FEM. In *Computing Methods in Applied Sciences and Engineering* (ed. R. Glowinski), pp. 373–382, Nova Science Publishers.

Heyman, J. (1966). The stone skeleton. *International Journal of Solids and Structures* **2,** 249–279.

Hilsdorf, H. K. (1969). Investigation into the failure mechanism of brick masonry loaded in axial compression. In *Designing, Engineering and Constructing with Masonry Products* (ed. F. B. Johnson), Proceedings of an International Conference on Masonry Structural Systems, Huston, Texas, pp. 34–41.

Kralj, B., Pande, G. N. and Middleton, J. (1991). On the mechanics of frost damage to brick masonry. *Computers and Structures* **41,** 53–66.

Laws, N., Dvorak, G. J. and Hejazi, M. (1983). Stiffness changes in unidirectional composites caused by crack systems. *Mechanics of Materials* **2,** 123–137.

Lofti, H. R. and Benson Shing, P. (1994). Interface model applied to fracture of masonry structures. *Journal of Structural Engineering, ASCE*, **120,** 63–80.

Luciano, R. (1995). Formulas for the bounds on the stiffness tensors of composite materials with periodic microstructure. Submitted for publication.

Luciano, R. and Sacco, E. (1995a). A micromechanical approach to the damage of the masonry material. In *Structural Studies, Repair and Maintenance of Historical Buildings* (eds B. Leftheris and C. A. Brebbia), Computational Mechanics Publications.

Luciano, R. and Sacco, E. (1995b). A numerical procedure for the analysis of masonry walls. To be published.

Mura, T. (1987). *Micromechanics of Defects in Solids*, Martinus Nijhoff Publishers.

Pande, G. N., Liang, J. X. and Middleton, J. (1989). Equivalent elastic moduli for brick masonry. *Computers and Geotechnology* **8,** 243–265.

Papa, E. (1990). Sulla meccanica del danneggiamento con particolare riferimento alle murature. Ph.D. thesis, Politecnico di Milano, Dipartimento di Ingegneria Strutturale.

Pietruszczak, S. and Niu, X. (1992). A mathematical description of macroscopic behaviour of brick masonry. *Computers and Geotechnology* **29,** 531–546.

Romano, G. and Sacco, E. (1987). Convex problems in structural analysis. In *Unilateral Problems in Structural Analysis* (eds G. Del Piero and F. Maceri), CISM Courses and Lectures, Vol. 304, pp. 279–297, Springer-Verlag, Berlin.

Sanchez-Hubert, J. and Sanchez-Palencia, E. (1992). *Introduction aux méthodes asymptotiques et a l'homogénéisation*, Masson.

Suquet, P. (1982). Plasticité et homogénéization. These de doctorat d'Etat, Université de Paris VI.

Talreja, R. (1987). *Fatigue of Composite Materials*, Technonic Publishing Co. Inc.

Teply, J. L. and Reddy, J. N. (1991). A unified formulation of micromechanics models of fiber-reinforced composites. In *Inelastic Deformation of Composite Materials* (ed. G. J. Dvorak), pp. 341–370, Springer-Verlag, Berlin.

Washizu, K. (1976). *Variational Methods in Elasticity and Plasticity*, Pergamon Press, Oxford.

Yim, C. S., Chopra, A. K. and Penzien, J. (1990). Rocking response of rigid blocks to earthquakes. *Earthquake Engineering and Structural Dynamics* **88,** 565–572.